International Journal of Pharmaceutical Research and Applications
Volume 10, Issue 2 Mar–Apr 2025, pp: 1845-1853 www.ijprajournal.com ISSN: 2456-4494

Rapid accelerated La doped Cu of eather like nanocomposites for antibacterial activity and catalytic eliminations of Rhodamine-B dye using sodium borohydride- conventional approach

M.S. Manoj Kumar[1*], G. Sasireka[2], C. Shivashankari[1], A. Harinika[3], P. Logeshwari[1].

[1]*Department of Biotechnology, Vivekanandha College of Engineering for Women, Namakkal, India.*
[2]*Department of Chemical Engineering, Hindustan College of Engineering and Technology, Coimbatore, India.*
[3]*Department of Computer Science and Engineering, M. Kumarasamy College of Engineering, Karur, India.*

Date of Submission: 15-04-2025 Date of Acceptance: 25-04-2025

ABSTRACT
Copper oxide (CuO) and lanthanum-doped CuO nanoparticles were synthesized and examined to study their structural, optical, morphological, antibacterial, and catalytic properties. This research evaluates the impact of lanthanum doping on these nanoparticles and highlights their enhanced performance. X-ray diffraction (XRD) confirmed a feather-like structure, while field emission scanning electron microscopy (FE-SEM) showed notable morphological changes due to La doping. Energy-dispersive X-ray (EDAX) analysis confirmed the chemical composition, and Fourier transform infrared (FTIR) spectroscopy verified the presence of Cu-O bonds, revealing a Cu-La-O stretching frequency at 445 cm^{-1}. The study found that increasing La doping positively influenced antibacterial activity, with La-doped CuO nanoparticles exhibiting superior effectiveness against both Gram-positive and Gram-negative bacteria compared to pure CuO. This enhancement was attributed to the release of reactive oxygen species (ROS) and Cu^{2+} ions. Additionally, La-doped CuO nanoparticles demonstrated excellent catalytic activity, achieving 99.9% degradation of rhodamine B dye in 8 minutes, showcasing their potential for environmental remediation.

KEYWORDS: La @ CuO NPs, Co-precipitation, Rhodamine B dye, FE-SEM

I. INTRODUCTION

Rhodamine B is a synthetic dye widely used in industries such as textiles, paper production, food processing, and scientific research, including fluorescence microscopy and flow cytometry. However, despite its widespread application, Rhodamine B poses significant environmental and health risks. As a persistent organic pollutant, its discharge into water bodies can lead to severe ecological damage, contaminating water sources and harming aquatic life. These potential hazards have heightened the demand for efficient methods to remove the dye from industrial wastewater. Simultaneously, the rise of bacterial infections, exacerbated by antibiotic-resistant strains, represents a growing public health challenge. The declining efficacy of traditional antibiotics highlights the urgent need for alternative antibacterial solutions. In this context, the development of materials with intrinsic antibacterial properties, such as nanoparticles, holds great promise for addressing both environmental pollution and microbial resistance.A type of nanomaterials known as metal oxide nanoparticles (NPs) is created extensively for usage in both domestic and industrial settings, and it has a great deal of room to grow. Since the first nanoecotoxicology study in 2006, bibliometric data show a growing body of research focusing on the environmental impacts of these NPs (A. Kahru& H.-C. Dubourguier 2010). Recently, copper oxide (CuO) and zinc oxide (ZnO) NPs, which are commonly used in industrial and household products, have been shown to negatively impact the survival and growth of various organisms (S. Nations et al., 2011). These findings raise concerns about the potential environmental risks associated with NP release.CuO, the simplest compound in the copper family, displays a variety of notable physical properties, including high-temperature superconductivity, electron correlation, and spin dynamics (R.J. Cava 1990; J.M. Tranquada et al., 1995). As a monoclinic semiconductor, it has gained significant attention for its photovoltaic and photoconductive properties, linked to its narrow band gap structure (J.F. Xu et al., 1999). Additionally, CuO NPs exhibit unique characteristics, such as enhancing fluid viscosity

International Journal of Pharmaceutical Research and Applications
Volume 10, Issue 2 Mar–Apr 2025, pp: 1845-1853 www.ijprajournal.com ISSN: 2456-4494

and thermal conductivity, making them valuable in energy-saving applications that improve energy conversion efficiency (P.K. Namburu et al., 2007). CuO NPs have found use in a wide range of fields, including gas sensors (A. Chowdhuri et al., 2004), catalysis (S. Jammi et al., 2009), batteries (D.-W. Zhang et al., 2005), high-temperature superconductors (M.A. Dar et al., 2008), solar energy conversion (M. Yin et al., 2005), and field emission devices (M.A. Dar et al., 2008). In industrial catalysis, CuO NPs show potential as a cost-effective substitute for carbon monoxide oxidation catalysts made of noble metals, offering reduced production costs and improved catalytic efficiency (K. Zhou et al., 2006).

In this study, La-doped CuO nanocomposites were synthesized via the co-precipitation method. The catalyst was characterized for its optical and crystalline properties and was tested for its effectiveness in catalyzing the degradation of Rhodamine B dye, as well as in antibacterial applications.

II. EXPERIMENTAL

2.1MATERIALS AND METHODS

All metal precursors, including copper(II) nitrate hexahydrate (Cu $(NO_3)_2 \cdot 6H_2O$), lanthanum nitrate hexahydrate ($La(NO_3)_3 \cdot 6H_2O$), sodium borohydride ($NaBH_4$), and sodium hydroxide pellets (NaOH), were sourced from Sigma-Aldrich Chemicals and were of analytical reagent (AR) grade. Additionally, a synthetic dye was obtained from textile industries. These chemicals were used as received, without further purification, for the synthesis of lanthanum-doped copper oxide nanoparticles. Double-distilled water was used throughout the experiments to ensure maximum purity and consistency in the results.

2.2 PREPARATION OF LA-DOPED CUO NANOCOMPOSITES

To synthesize La-doped CuO nanocomposites, 0.095 M of copper nitrate hexahydrate, 0.005 M of lanthanum nitrate hexahydrate, and 0.8 M of sodium hydroxide (NaOH) were each dissolved in 400 ml of distilled water in separate 500 ml beakers. First, the copper nitrate and lanthanum nitrate solutions were mixed thoroughly to ensure homogeneity. Then, the NaOH solution was slowly added dropwise to the mixture, forming a black precipitate. This mixture was stirred at room temperature for 30 minutes before being heated to 60 °C for 4 hours. The solution was then refluxed at room temperature for 24 hours, resulting in a clear and stable solution. The precipitate was washed multiple times with double-distilled water, followed by ethanol, to eliminate impurities. The La-doped CuO sample was then obtained by drying the precipitate at 120 °C. To improve crystallinity, the sample was annealed at 600 °C for 4 hours, enhancing atomic vibrations and diffusion, which promoted the formation of well-defined crystalline structures in the La-doped CuO nanocomposites.

2.3CATALYTIC DYE ELIMINATION TEST

The catalytic elimination of rhodamine dye was performed using lanthanum-doped copper oxide (La-doped CuO) nanoparticles and sodium borohydride ($NaBH_4$). Initially, 50 mL of 10 mg/L rhodamine dye solution was placed into a 100 mL beaker. Subsequently, 1 mL of 0.1 M $NaBH_4$ solution was added to this mixture.

Following this, 10 mg of La-doped CuO nanoparticles were thoroughly mixed into the solution while maintaining constant stirring to ensure uniform dispersion of the nanoparticles. The degradation efficiency of the catalyst was calculated using the following formula

$$\text{Degradation Efficiency} \quad (\%) = C_0 - C_t / C_0 \times 100 \quad (1)$$

where C_0 is the initial concentration of the rhodamine dye and C_t is the concentration at time t.

IV. RESULTS AND DISCUSSION

3.1XRD STUDIES

The X-ray diffraction (XRD) patterns of both pure and La-doped CuO nanoparticles (NPs) annealed at 600°C are shown in Figure 1. The peaks in the XRD pattern reveal a well-crystallized monoclinic phase of CuO NPs, consistent with JCPDS data for the C2/c space group (card number: 48-1548). There was no impurity peaks found, such as those connected to Cu $(OH)_2$, Cu_2O, or Cu. confirming the absence of any impurities from plant extracts. Furthermore, no noticeable peak shifts were observed in the La-doped CuO NPs, indicating successful integration of La into the CuO matrix. The particle size of the synthesized CuO NPs was determined using X-ray line broadening and Scherrer's equation.

$$D = 0.9\lambda / \beta\cos\theta \quad (1)$$

Where D represents the particle size in nanometers, λ is the wavelength of the radiation (1.5406 Å for Cu Kα), k is a constant (0.94), β is the peak width at half-maximum intensity, and θ is the peak position. The average crystallite size of the synthesized CuO NPs is 32 nm, whereas the

International Journal of Pharmaceutical Research and Applications
Volume 10, Issue 2 Mar–Apr 2025, pp: 1845-1853 www.ijprajournal.com ISSN: 2456-4494

La-doped CuO NPs have an average size of 23 nm. The reduction in particle size and the observed changes in shape are attributed to the incorporation of La into the CuO matrix.

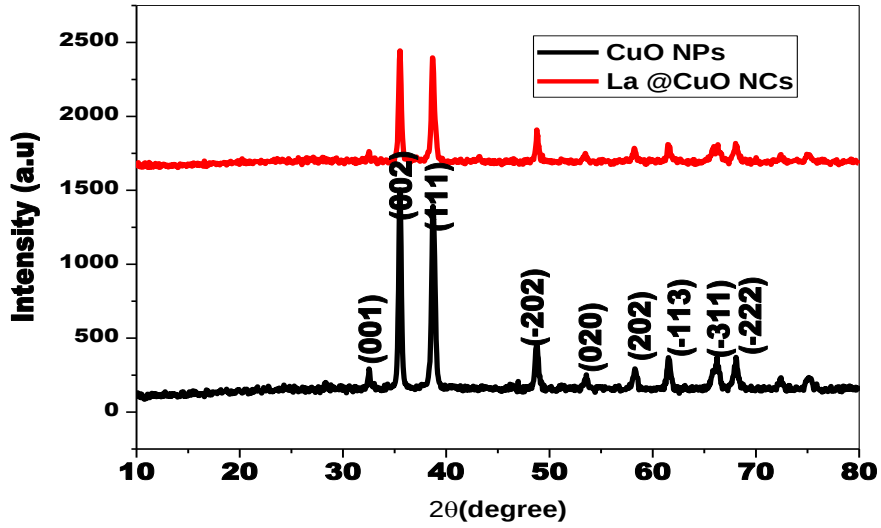

Fig: 1.X-ray powder diffraction patterns of pure and La doped CuO NPs

3.2MORPHOLOGICAL ANALYSES

Fig: 2 (a) SEM image of Pure CuO NPs (b) SEM image of La@CuO NPs (c) EDX Profile of Pure CuO NPs (d) EDX Profile of La@CuO NPs

International Journal of Pharmaceutical Research and Applications
Volume 10, Issue 2 Mar–Apr 2025, pp: 1845-1853 www.ijprajournal.com ISSN: 2456-4494

The morphologies of CuO and La-doped CuO NPs were examined using field emission scanning electron microscopy (FESEM). Scanning electron microscopy (SEM) of CuO nanoparticles reveals that they primarily form irregular nanoplatelets, as shown in Fig. 2(a). The SEM images clearly depict the surface features, indicating that the CuO nanoparticles were successfully synthesized, with particles clustering together and an average size of approximately 100 nm. Fig. 2(b) presents FESEM images of the La-doped CuO nanoparticles, which exhibit a distinctive feather-like morphology. The transformation from irregular nanoplatelets to feather-like particles confirms the successful incorporation of La into the CuO crystal structure. The chemical compositions of Cu and O in the pure CuO NPs are 60.99% and 39.01%, respectively (Fig. 2(c)). In the La-doped CuO sample, the compositions of Cu, La, and O are 58.93%, 3.14%, and 37.93%, respectively (Fig. 2(d)).

3.3 TEM/HRTEM AND SAED PATTERN

Fig: 3 (a) and (b) different resolution of La@CuONPs (c) HRTEM image (d) SAED pattern

La-doped CuO nanocrystals (NCs) were thoroughly examined using Transmission Electron Microscopy (TEM), High-Resolution Transmission Electron Microscopy (HRTEM), and Selected Area Electron Diffraction (SAED). TEM analysis, shown in Fig. 3(a), revealed that the nanocrystals had a spherical morphology with an average size of 32 nm. HRTEM imaging, displayed in Fig. 3(c), showed clear lattice fringes with a spacing of 0.213 nm, indicating the high crystallinity and well-ordered structure of the nanocrystals. These observations were further confirmed by the SAED pattern (Fig. 3(d)), which validated the crystalline nature of the La-doped CuO NCs.

3.4 FT-IR STUDIES

FTIR spectroscopy (Fig. 4(a)) was employed to validate the XRD line profile analysis and assess the purity of both pure and La-doped CuO nanoparticles. As shown in Fig. 4(a), peaks at 3422 cm^{-1} and 1610 cm^{-1} are attributed to the stretching and bending vibrations of the O-H group, respectively (A. Goswami et al., 2012). Peaks at 2814 cm^{-1} and 1365 cm^{-1} are associated with C-H stretching vibrations and physiosorbed

International Journal of Pharmaceutical Research and Applications
Volume 10, Issue 2 Mar–Apr 2025, pp: 1845-1853 www.ijprajournal.com ISSN: 2456-4494

H_2O molecules on the surface of the nanostructured CuO NPs (K. Karthik et al., 2011). Absorption peaks in the range of 400-850 cm^{-1} are related to Cu-O and La-O-Cu lattice vibrations. Specifically, peaks at 769, 613, and 497 cm^{-1} correspond to the characteristic stretching vibrations of the Cu-O bond in monoclinic CuO(I.Y. Erdogan & O. Gullu 2010).

Fig: 4(a) FT-IR and (b) UV spectra of the pure and La doped CuO NPs

3.5UV-VISIBLE SPECTROSCOPIC STUDIES

UV-Visible absorption spectroscopy is a crucial method for examining the optical properties of chemically synthesized CuO nanoparticles. The absorption spectrum for these nanoparticles is displayed in Figure 4b. It shows that the absorption peaks for both pure and La-doped CuO nanoparticles are at 232 nm and 235 nm, respectively, which is shorter than the absorption peak for bulk CuO at 310 nm (X. Zhang et al., 2008). Additionally, Figure 4b illustrates a noticeable blue shift in the pure CuO NPs, which can be attributed to the quantum confinement effect of the nanoparticles

$$\alpha h\upsilon = A(h\upsilon - E_g)^n \qquad (2)$$

Here, EgE_gEg represents the optical band gap, α\alphaα is the absorption coefficient, AAA is a constant, and nm is an exponent that depends on the type of electronic transition. The value of nm can be 1/2, 3/2, 2, or 3, depending on the nature of the transition: n=1/2n = 1/2n=1/2 for permitted straight transitions, n=2n = 2n=2 for permitted secondary transitions, n=3/2n = 3/2n=3/2 for forbidden direct transitions, and n=3n = 3n=3 for forbidden indirect transitions.

3.6ANTIBACTERIAL ACTIVITY

Fig. 5(a) illustrates the CuO nanoparticles zone of inhibition against both Gram-negative bacteria (Escherichia coli, Pseudomonas aeruginosa) at various concentrations (1, 3, and 5 mg/ml) and Gram-positive bacteria (Streptococcus pneumoniae, Staphylococcus aureus). The results clearly demonstrate that copper oxide nanoparticles effectively inhibit the growth of both types of bacteria, with the zone of inhibition expanding as the concentration of nanoparticles increases, as detailed in Table 1.

International Journal of Pharmaceutical Research and Applications
Volume 10, Issue 2 Mar–Apr 2025, pp: 1845-1853 www.ijprajournal.com ISSN: 2456-4494

Table: 1Zone of inhibition of $Cu_{1-x}La_xO$nanoparticles against bacterial strains

	Gram + ve		Gram - ve	
Compound	**Staphylococcus aureus**	**Streptococcus pneumonia**	**Escherichia coli**	**Pseudomonas aeruginosa**
30 (CuO)	7	8	7	12
40	8	9	7	12
50	8	9	7	12
Amoxycillin	6	7	7	7
30 (CuO:La)	10	12	11	10
40	10	10	11	10
50	11	10	12	11
Amoxycillin	9	7	10	6

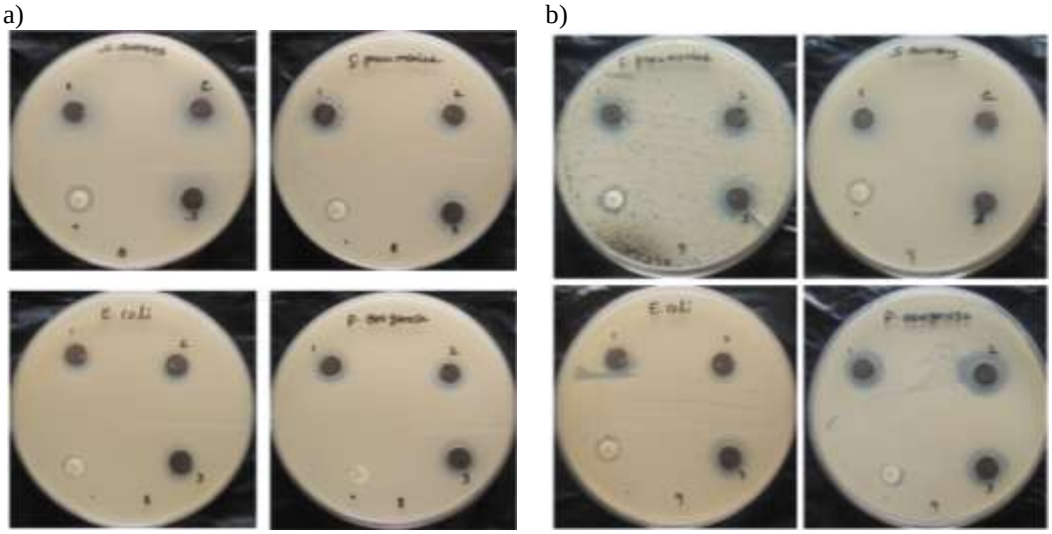

Fig: 5Zone of inhibition of (a) pure and (b) La doped Copper oxide nanoparticles

The antibacterial activities of pure and La-doped CuO NPs at three different concentrations (1 mg/ml, 3 mg/ml, and 5 mg/ml) were tested against the pathogens Gram-negative E. coli and Gram-positive S. aureus. The zone of inhibition's size and the CuO NPs' antibacterial effectiveness against these bacterial pathogens are shown in Fig. 5(a) and 5(b). As shown in Table 1, La-doped CuO nanoparticles demonstrated a strong antibacterial effect on every pathogen tested. Gram-positive and Gram-negative bacteria differ in their adaptability and rebellion, which can be explained by variations in their cell physiology, structure, metabolism, or degree of contact with the nanoparticles. The effectiveness of CuO NPs as an antimicrobial is primarily influenced by the existence of ROS (reactive oxygen species), which are enhanced by factors such as smaller particle size, reduced agglomeration, better diffusion of reactant molecules (O. Yamamoto et al., 2004), increased lattice constant, and morphology. Additionally, the electrostatic attraction between the negatively charged bacterial cells and the positively charged nanoparticles plays a critical role in their bactericidal activity. This interaction not only inhibits bacterial growth but also promotes the generation of ROS, leading to cell death.

The nanoparticles interact with bacterial cell walls and penetrate into the cells (C. Karunakaran et al., 2010). Once inside, they may induce intracellular oxidative stress by disrupting the balance between oxidants and antioxidants. This oxidative stress can increase cytosolic calcium levels or trigger the translocation of transcription factors to the nucleus, which regulates pro-inflammatory genes. Excessive oxidative stress may also alter proteins, lipids, and nucleic acids, stimulating the antioxidant defense system or causing cell death (Xiaoke Hu et al., 2009).

International Journal of Pharmaceutical Research and Applications
Volume 10, Issue 2 Mar–Apr 2025, pp: 1845-1853 www.ijprajournal.com ISSN: 2456-4494

3.7 CATALYTIC ELIMINATION OF RHODAMINE -B DYE

Fig: 6 (a) catalytic degradation of Rhodamine -B (b) Kinetic plot

Fig. 6(a) demonstrates the catalytic elimination of Rhodamine B dye using La-doped CuO nanoparticles in the presence of sodium borohydride. Initially, the dye alone showed minimal degradation. However, when a small amount of sodium borohydride was added, a decrease in the absorption curve indicated partial reduction of the dye. The introduction of La-doped CuO nanoparticles significantly accelerated the degradation process, achieving a 99.9% elimination of Rhodamine B within 7 minutes. This exceptional efficiency is attributed to the electron relay effect, which enhances the reduction process. Fig. 6(b) shows that the reaction follows pseudo-first-order kinetics and occurs efficiently without the need for light activation.

3.8CATALYTIC ELIMINATION MECHANISM

Fig: 7 catalytic elimination mechanism of La @CuONPs upon rhodamine dye using $NaBH_4$

International Journal of Pharmaceutical Research and Applications
Volume 10, Issue 2 Mar–Apr 2025, pp: 1845-1853 www.ijprajournal.com ISSN: 2456-4494

The reduction of dyes by La-doped CuO nanoparticles (NPs) is facilitated through an electron transfer mechanism, as illustrated in Fig. 7. The La-doped CuO NPs act as efficient conductors, enabling electron transfer between donors and acceptors. In this catalytic process, NaBH4 initiates the reduction of Rhodamine B dye in the presence of La-doped CuO NPs. Electrons are transferred from $BH4^-$ ions to the dye, resulting in the reduction of Rhodamine B to a colorless form by removing its chromophore groups. Initially, $BH4^-$ ions donate electrons to the La-doped CuO NPs, creating a negatively charged layer around them. This layer enhances electron transfer to the positively charged dye molecules through electrostatic interactions. As a cationic dye, Rhodamine B is strongly attracted to the negatively charged La-doped CuO NPs, facilitating rapid electron transfer and reduction to a colorless state. Additionally, NaBH4 provides hydrogen, which aids in the degradation of the dye. The reduced dye then desorbs from the NP surface and diffuses into the solution due to weaker electrostatic interactions with the degradation products.

V. CONCLUSION

The widespread applications of nanotechnology across material sciences, biology, chemistry, and medicine have demonstrated the significant potential of nanoparticles as powerful tools in various aspects of human life. Nanoparticles with antibacterial properties hold immense promise for food preservation and the development of antibacterial surfaces. The antibacterial effects of nanoparticles span a broad range of materials, including metals and metal oxides. A key aspect of their successful application as antibacterial agents is the sustained release of active substances into the environment. However, it is crucial to consider the potential toxicity and safe use of nanoparticles to ensure their beneficial impact. La-doped CuO nanocomposites, in particular, exhibit multifunctionality, making them suitable for diverse applications such as in textile industries and the treatment of bacterial infectious diseases. Their enhanced antibacterial properties, coupled with their catalytic efficiency in degrading environmental pollutants, underscore their potential as versatile and effective tools in both industrial and medical fields.

Acknowledgments

The authors are thankful to the Principal and the Management of Vivekanandha College of Arts and Sciences for Women (Autonomous) for providing necessary facilities.

Conflict interest

The author declared no conflict interest.

REFERENCES

[1]. Kahru, H.-C. Dubourguier, From ecotoxicology to nanoecotoxicology. Toxicology **269**, 105–119 (2010).
[2]. S. Nations, M. Wages, J. E. Cañas, J. Maul, C. Theodorakis, G.P. Cobb, Acute effects of Fe2O3, TiO2, ZnO and CuO nanomaterials on Xenopus laevis. Chemosphere **83**, 1053–1061 (2011).
[3]. R.J. Cava, Structural chemistry and the local charge picture of copper oxide superconductors. Science **247**, 656–662 (1990).
[4]. J.M. Tranquada, B.J. Sternlieb, J.D. Axe, Y. Nakamura, S. Uchida, Evidence for stripe correlations of spins and holes in copper oxide superconductors. Nature **375**, 561–563 (1995).
[5]. J.F. Xu, W. Ji, Z.X. Shen, S.H. Tang, X.R. Ye, D.Z. Jia, X.Q. Xin, Preparation and characterization of CuO nanocrystals. J. Solid State Chem. **147**, 516–519 (1999).
[6]. P.K. Namburu, D.P. Kulkarni, D. Misra, D.K. Das, Viscosity of copper oxide nanoparticles dispersed in ethylene glycol and water mixture. Exp. Therm. Fluid Sci. **32**, 397–402 (2007).
[7]. A.Chowdhuri, V. Gupta, K. Sreenivas, R. Kumar, S. Mozumdar, P.K. Patanjali, Response speed of SnO2-based H2S gas sensors with CuO nanoparticles. Appl. Phys. Lett. **84**, 1180–1182 (2004).
[8]. S. Jammi, S. Sakthivel, L. Rout, T. Mukherjee, S. Mandal, R. Mitra, P. Saha, T. Punniyamurthy, CuO nanoparticles catalyzed C-N, C-O, and C-S cross-coupling reactions: Scope and mechanism. J. Org. Chem. **74**, 1971–1976 (2009).
[9]. D.-W. Zhang, T.-H. Yi, C.-H. Chen, Cu nanoparticles derived from CuO electrodes in lithium cells. Nanotechnology **16**, 2338–2341 (2005).
[10]. M.A. Dar, Y.S. Kim, W.B. Kim, J.M. Sohn, H.S. Shin, Structural and magnetic properties of CuO nanoneedles

synthesized by hydrothermal method. Appl. Surf. Sci. **254**, 7477–7481 (2008).

[11]. M. Yin, C.-K. Wu, Y. Lou, C. Burda, J.T. Koberstein, Y. Zhu, S. O'Brien, Copper oxide nanocrystals. J. Am. Chem. Soc. **127**, 9506–9511 (2005).

[12]. K. Zhou, R. Wang, B. Xu, Y. Li, Synthesis, characterization and catalytic properties of CuO nanocrystals with various shapes. Nanotechnology **17**, 3939–3943 (2006).

[13]. A.Goswami, PK. Raul, M.K. Purkait, Arsenic adsorption using copper (II) oxide nanoparticles, Chem. Eng. Res. Des., **90**(9), 1387-1396 (2012).

[14]. K. Karthik, N. Victor Jaya, M. Kanagaraj, S. Arumugam, Temperature-dependent magnetic anomalies of CuO nanoparticles, Solid State Commun., **151**(7), 564-568 (2011).

[15]. I.Y. Erdogan, O. Gullu, Optical and structural properties of CuO nanofilm: Its diode application, J. Alloys. Compd., **492**(1-2), 378-383 (2010).

[16]. X. Zhang, D. Zhang, X. Ni, H. Zheng, Optical and electrochemical properties of nanosized CuO via thermal decomposition of copper oxalate, Solid State Electron., **52**(2), 245-248 (2008).

[17]. O. Yamamoto, M. Komatsu, J. Sawai, E.Z. Nakagawa, Effect of lattice constant of zinc oxide on antibacterial characteristics, J. Mater. Sci. Mater. Med., **15**(8), 847-851 (2004).

[18]. Karunakaran, P. Gomathi Sankar, G. Manikandan, Preparation and characterization of antimicrobial Ce-doped ZnO nanoparticles for photocatalytic detoxification of cyanide, Mater. Chem. and Phys., **123**(2-3), 585-594 (2010).

[19]. Xiaoke Hu, Sean Cook, Peng Wang, Huey-min Hwang, In vitro evaluation of cytotoxicity of engineered metal oxide nanoparticles, Sci. Total Environ., **407**(8), 3070–3072 (2009).